[3] M. Argyropoulou, S. Fanis, T. Xenakis, S. Efremidis, and A. Siamopoulou, "The role of MRI in the evaluation of hip joint disease in clinical subtypes of juvenile idiopathic arthritis," *Br. J. Radiol.*, vol. 75, pp. 229–233, 2002.
[4] J. S. de Gauzy, N. Kerdiles, C. Baunin, J. Kany, P. Darodes, and J. Cahuzac, "Imaging evaluation of subluxation in legg-calvéperthes disease: magnetic resonance imaging compared with the plain radiograph," *J. Pediatr. Orthop.*, vol. 6, pp. 235–238, 1997.
[5] G. Sebag, S. Lamer, N. Belarbi, and M. Hassan, "Advances in imaging of legg-calvé-perthes disease," *ESPR, Syllabus. Pediatric Radiology*, pp. 61–64, May 2000.
[6] H. Hawighorst *et al.*, "Evaluation of angiogenesis and perfusion of bone marrow lesions: role of semiquantitative and quantitative dynamic MRI," *J. Magn. Reson. Imag.*, vol. 10, pp. 286–294, 1999.
[7] K. Verstraete and P. Lang, "Bone and soft tumors: the role of contrast agents for MR imaging," *Eur. J. Radiol.*, vol. 34, pp. 229–246, 2000.
[8] J. Herring and J. Neustadt *et al.*, "The lateral pillar classification of Legg-Calvé-Perthes Disease," *J. Pediatr. Orthop.*, vol. 12, no. 2, pp. 143–150, 1992.
[9] B. Chaudhuri and N. Sarkar, "Texture segmentation using fractal dimension," *IEEE Trans. Pattern Anal. Mach. Intell.*, vol. 17, no. 1, pp. 72–77, Jan. 1995.
[10] R. Haralick, K. Shanmugam, and I. Distein, "Textural features for image classification," *IEEE Trans. Syst., Man, Cybern.*, vol. SMC-3, no. 6, pp. 610–621, 1973.
[11] M. Galloway, "Texture analysis using gray level run lengths," *Comput. Graphic. Image Process.*, vol. 4, pp. 172–179, 1975.
[12] A. Chu, C. Seghal, and J. F. Greenleaf, "Use of gray value distribution of run length for feature analysis," *Pattern Recognit. Lett.*, vol. 11, pp. 415–420, 1990.
[13] A. Gagalowicz, "Vers un Modèle de Texture," Master's thesis, Université Pierre et Marie Curie, Paris, France, 1983.
[14] K. Laws, "Textured Image Segmentation," Master's thesis, Univ. Southern California, Los Angeles, Jan. 1980.
[15] J. A. Maintz and M. Viergever, "A survey of medical image registration," *Med. Image Anal.*, vol. 2, no. 1, pp. 1–36, 1998.
[16] B. Dasarathy, *Nearest Neighbor (NN) Norms: NN Pattern Classification Techniques*. Los Alamitos, CA: IEEE Computer Soc. Press, 1991.
[17] S. Raudys and A. K. Jain, "Small sample size effects in statistical pattern recognition: recommendations for practitioners," *IEEE Trans. Pattern Anal. Mach. Intell.*, vol. 13, no. 3, pp. 252–264, Mar. 1991.
[18] S. Herlidou, R. Grebe, F. Grados, N. Leuyer, P. Fardellone, and M. Meyer, "Influence of age and osteoporosis on calcaneus trabecular bone structure: a preliminary *in vivo* MRI study by quantitative texture analysis," *Magn. Reson. Imag.*, vol. 22, pp. 237–243, 2004.
[19] S. Herlidou, Y. Rolland, J. Bansard, E. L. Rumeur, and J. de Certaines, "Comparison of automated and visual texture analysis in MRI: characterization of normal and diseased skeletal muscle," *Magn. Reson. Imag.*, vol. 17, pp. 1393–1397, 1999.
[20] J. Bézy-Wendling, M. Kretowski, Y. Rolland, and W. L. Bidon, "Toward a better understanding of texture in vascular CT scan simulated images," *IEEE Trans. Biomed. Eng.*, vol. 48, no. 1, pp. 120–124, Jan. 2001.
[21] J. Boss and I. Misselevich, "Experimental avascular osteonecrosis," *Curr. Orthop.*, vol. 15, pp. 57–67, 2001.
[22] S. Chung, "The arterial supply of the developing proximal end of the human femur," *J. Bone Joint Surg.*, vol. 58, no. 7, pp. 961–970, 1976.
[23] G. Collewet, M. Strzelecki, and F. Mariette, "Influence of MRI acquisition protocols and image intensity normalization methods on texture classification," *Magn. Reson. Imag.*, vol. 22, pp. 81–91, 2004.
[24] K. L. Verstraete, H. J. Van der Woude, P.C. Hogendoorn, Y. De-Deene, M. Kunnen, and J. L. Bloem, "Dynamic contrast-enhanced MR imaging of musculoskeletal tumors: basic principles and clinical applications," *J Magn. Reson. Imag.*, vol. 6, pp. 311–321, 1996.
[25] B. Nielsen, F. Albregtsen, and H. Danielsen, "Low dimensional adaptive texture feature vectors from class distance and class difference matrices," *IEEE Trans. Med. Imag.*, vol. 23, no. 1, pp. 73–84, Jan. 2004.

A Robust Method for Spike Sorting With Automatic Overlap Decomposition

Guang-Li Wang, Yi Zhou, Ai-Hua Chen, Pu-Ming Zhang, and Pei-Ji Liang*

***Abstract*—Spike sorting is the mandatory first step in analyzing multiunit recording signals for studying information processing mechanisms within the nervous system. Extracellular recordings usually contain overlapped spikes produced by a number of neurons adjacent to the electrode, together with unknown background noise, which in turn induce some difficulties in neural signal identification. In this paper, we propose a robust method to deal with these problems, which employs an automatic overlap decomposition technique based on the relaxation algorithm that requires simple fast Fourier transforms. The performance of the presented system was tested at various signal-to-noise ratio levels based on synthetic data that were generated from real recordings.**

***Index Terms*—FFTs, RELAX, spike sorting.**

I. Introduction

The detection and classification of neural spike activity from multiunit recordings in the presence of background noise with unknown properties, a problem commonly referred to as spike sorting, is the mandatory first step in studying information processing mechanisms within the nervous system [1].

Methods of spike sorting have been extensively studied during the past decades and a large number of techniques and related problems have been summarized [2], but their applications are severely limited by some unsolved problems. First, *a priori* assumption about background noise cannot accurately capture its statistical characteristics [3]. Second, overlapping of action potentials fired by adjacent neurons will complicate spike identification. Although some algorithms considering the overlapping problem have been proposed [4]–[7], these methods were all with the restraint that the background noise properties were known *a priori*.

In this paper, a robust method is developed to deal with these problems simultaneously. In order to identify those ambiguous waveforms that contain overlapping spike events and severely distorted spike waveforms, model analysis is performed and cost functions are calculated for all possible templates or combinations of spike waveforms in the frequency domain. For minimizing the cost function that contains a number of unknown parameters, an approach based on a decoupled parameter estimation algorithm—the relaxation (RELAX) algorithm [8], which is originated from the cyclic minimization [9] and has been applied in radar signal processing [8], [10], is implemented. This algorithm requires simple fast Fourier transforms (FFTs), and can be

Manuscript received January 14, 2005; revised October 29, 2005. This work was supported inpart by the National Basic Research Program of China under Grant 2005CB724301, in part by the National Natural Science Foundation of China under Grant 30400088, and in part by the Ministry of Education of China under Grant 20040248062. *Asterisk indicates corresponding author.*

G.-L. Wang, Y. Zhou, and P.-M. Zhang are with the Department of Biomedical Engineering, Shanghai Jiao Tong University, Shanghai 200030, China (e-mail: wglsx@sjtu.edu.cn).

*P.-J. Liang is with the Department of Biomedical Engineering, Shanghai Jiao Tong University, Shanghai 200030, China (e-mail: pjliang@sjtu.edu.cn).

A.-H. Chen is with Shanghai Institutes for Biological Sciences, Chinese Academy of Sciences, Shanghai 200031, China.

Digital Object Identifier 10.1109/TBME.2006.873397

easily implemented on computer. The spike template or the combination of spike templates, which is corresponding to the minimum of the minimized cost functions for all possible combinations, is assigned as the best fitting to the waveform being examined. This process is robust to background noise, because no assumptions about noise properties are requested.

II. Method

A. Feature Extraction and Templates Reconstruction

In this study, feature extraction and template reconstruction basically follow that explained in a previous report [5]. In brief, principal component analysis (PCA) is used to extract feature from the data set that consists of events to be classified which are detected using a nonlinear energy operator [11]. The scores of the first three principal components serve as the feature for spike events classification. A subtractive clustering technique is then employed to determine the number of the clusters, as well as the initial values of the cluster centers, by analyzing the feature, and the K-means algorithm is further used to optimize the cluster centers. The spike events corresponding to the data points contained in the spherical areas whose radius is determined by the minimal of the distances between each pair of cluster centers are regarded as classified spikes, and others are considered as unclassified ones which will be classified or decomposed in the subsequent process. The template for each neuron is then reconstructed by averaging the spike waveforms that fall within each spherical cluster.

B. Automatic Overlap Decomposition Based on the RELAX Algorithm via FFTs

The unclassified spike events that contain overlapping ones and severely distorted ones can be modeled as follows:

$$y(n) = \sum_{m=1}^{M} s_m(n+\tau_m) + \varepsilon(n) \tag{1}$$

where $m = 1, 2, \ldots, M$ represents the possible number of neurons contributing to the waveform to be classified; $s_m(n)$ stands for the estimated template which is reconstructed based on the classified spikes; τ_m reflects the relative time delay of the mth reconstructed template; $\varepsilon(n)$, $n = 1, 2, \ldots, N$ is the background noise with unknown properties. N denotes the number of data samples included in each single waveform. Let $Y(\omega_k)$, $S_m(\omega_k)$, and $E(\omega_k)$ denote the Fourier transforms of $y(n)$, $s_m(n)$, and $\varepsilon(n)$ at a certain frequency ω_k, respectively, where $k = 1, 2, \ldots, K$ represents the frequency index. In this case, the time domain data model (1) can alternatively be formulated in the frequency domain as

$$Y(\omega_k) = \sum_{m=1}^{M} S_m(\omega_k) e^{j\omega_k \tau_m} + E(\omega_k). \tag{2}$$

We form the following cost function using the integrated noise spectrum based on M templates

$$C\left(\{\tau_m\}_{m=1}^{M}\right) = \sum_{k=1}^{K} \left| Y(\omega_k) - \sum_{m=1}^{M} S_m(\omega_k) e^{j\omega_k \tau_m} \right|^2. \tag{3}$$

Minimizing $C(\{\tau_m\}_{m=1}^{M})$ with respect to the unknown parameters $\{\tau_m\}_{m=1}^{M}$ is a highly nonlinear optimization problem. Therefore, an approach based on the RELAX algorithm [8] is presented in this study.

Let

$$Y_m(\omega_k) = Y(\omega_k) - \sum_{i=1, i\neq m}^{M} S_i(\omega_k) e^{j\omega_k \hat{\tau}_i} \tag{4}$$

and

$$\mathrm{g}_m = \sum_{k=1}^{K} \left| Y_m(\omega_k) - S_m(\omega_k) e^{j\omega_k \tau_m} \right|^2 \tag{5}$$

where $\{\hat{\tau}_i\}_{i=1, i\neq m}^{M}$ are assumed to be given. In order to estimate τ_m based on the minimized cost function (5), we can express the problem as

$$\min_{\tau_m}(\mathrm{g}_m) = \min_{\tau_m} \sum_{k=1}^{K} \left| Y_m(\omega_k) - S_m(\omega_k) e^{j\omega_k \tau_m} \right|^2. \tag{6}$$

Equation (6) can be rewritten as

$$\hat{\tau}_m = \arg\min_{\tau_m} \sum_{k=1}^{K} \left| Y_m(\omega_k) - S_m(\omega_k) e^{j\omega_k \tau_m} \right|^2. \tag{7}$$

The solution to the minimization problem can thus be presented as

$$\hat{\tau}_m = \arg\min_{\tau_m} \left\{ \sum_{k=1}^{K} \left[|Y_m(\omega_k)|^2 + |S_m(\omega_k)|^2 \right] - 2 \times \mathrm{Re} \sum_{k=1}^{K} \left[Y_m(\omega_k) S_m^*(\omega_k) e^{-j\omega_k \tau_m} \right] \right\}. \tag{8}$$

Since $Y_m(\omega_k)$ and $S_m(\omega_k)$ are independent of parameter τ_m, the minimization of the cost function with respect to τ_m can be determined efficiently as follows:

$$\hat{\tau}_m = \arg\max_{\tau_m} \left\{ \mathrm{Re} \sum_{k=1}^{K} \left[Y_m(\omega_k) S_m^*(\omega_k) e^{-j\omega_k \tau_m} \right] \right\}. \tag{9}$$

Hence, $\hat{\tau}_m$, $m = 1, 2, \ldots, M$ is obtained as the location of the dominant peak of $\mathrm{Re} \sum_{k=1}^{K} [Y_m(\omega_k) S_m^*(\omega_k) e^{-j\omega_k \tau_m}]$, which can be efficiently computed by applying the FFT, using the sequence $[Y_m(\omega_k) S_m^*(\omega_k)]$ padded with zeros as input.

With the above preparations, we can describe the steps of the approach based on the RELAX algorithm as follows.

Step 1) Let $M = 1$. Obtain $\hat{\tau}_1$ from (4) and (9), and calculate the cost function by using (3).

Step 2) Let $M = 2$. Compute $Y_2(\omega_k)$ with (4) by using $\hat{\tau}_1$. Obtain $\hat{\tau}_2$ from $Y_2(\omega_k)$ by using (9). Next, compute $Y_1(\omega_k)$ with (4) by using $\hat{\tau}_2$, and re-determine $\hat{\tau}_1$ from $Y_1(\omega_k)$ by using (9).
Iterate Step 2) until "practical convergence" is achieved, and calculate the cost function by using (3).

Step 3) Let $M = 3$. Compute $Y_3(\omega_k)$ with (4) by using $\{\hat{\tau}_i\}_{i=1,2}$. Obtain $\hat{\tau}_3$ from $Y_3(\omega_k)$ by using (9). Next, compute $Y_1(\omega_k)$ by using $\{\hat{\tau}_i\}_{i=2,3}$ and re-determine $\hat{\tau}_1$ from $Y_1(\omega_k)$. Then compute $Y_2(\omega_k)$ by using $\{\hat{\tau}_i\}_{i=1,3}$ and re-determine $\hat{\tau}_2$ from $Y_2(\omega_k)$.

Iterate Step 3) until "practical convergence" is achieved, and finally, calculate the cost function by using (3).
Remaining Steps: Continue similarly until M is equal to the pre-determined number of reconstructed templates T.

The "practical convergence" in the iterations of the above approach based on the RELAX algorithm can be determined by checking the relative change of the cost function in (3) between the two consecutive iterations.

Using the above method, the algorithm yields values of the minimized cost functions for all the possible templates or template combinations. The template or template combination corresponding to the minimum of all the minimized cost functions reflects the optimal classification of the spike event examined.

III. Results and Discussions

Synthetic data have some advantages over real data in evaluating the performance of algorithms, since the exact information such as the number of the spike classes and the firing times of each spike can be known in advance.

First, synthetic data were constructed using three spike waveforms recorded from chicken retinal ganglion cells [12] together with a segment of real background noise [5]. Each template waveform lasted for 2 ms (40 sampling points, 16 points before and 23 points after the peak point). In order to construct the synthetic data, each template was superposed respectively with a segment of random background noise. This procedure was repeated for 500 times, which yielded totally 1500 spike waveforms distorted by background noise. Each two of the three templates were then superposed with each other with random time delays, together with a segment of random background noise. Fifty repeats resulted in a total number of 150 combinations. Finally, all of the three templates were superposed with random time delays and a segment of random background noise, with 50 repeats. All of the synthetic overlapping spikes are shown in Fig. 1. Although there are many ways of defining the signal-to-noise ratio (SNR), we define it as [13]

$$\mathrm{SNR} = \left(\frac{\mathrm{root-mean-square\ value\ of\ action\ potential\ waveform}}{\mathrm{root-mean-square\ value\ of\ pure\ noise\ segment}}\right)^2.$$

In the experiments, the sampling frequency is 20 kHz and the number of frequency K is selected as 4096 considering the quick implementation of FFT and the spectra of spikes. The SNR was tuned by amplifying the real background noise by a desired factor. The system's performance was tested at various SNR levels as illustrated by Fig. 2(a). Notice that the correct classification ratio of all single spikes is over 95% and the correct decomposition ratio of overlapping spikes is over 80%, under the situation that SNR is over 2.4. Since in our experimental data, superposition of two waveforms is more frequently detected than the superposition of more spikes, we examined the system's performance based on the presence of two templates (I and II given in Fig. 1). The results are given in Fig. 2(b). It is clear that the results are better than those for the three-class case. The correct classification ratio of all single spikes is nearly 100% and the correct decomposition ratio of overlapping spikes is over 95%, when SNR is over 2.4. Similar results can also be obtained when overlapping occurs between templates II/III and templates I/III.

When spike sorting is performed, background noise is always an important issue. It is true that the proposed RELAX algorithm will be spoiled when the SNR drops to be less than 2.0. However, in our experiments, more often than not, the SNR is around a reasonable level at 2.5. On the other hand, it is also true that the performance of PCA will decrease when SNR reduces. However, the templates can be properly

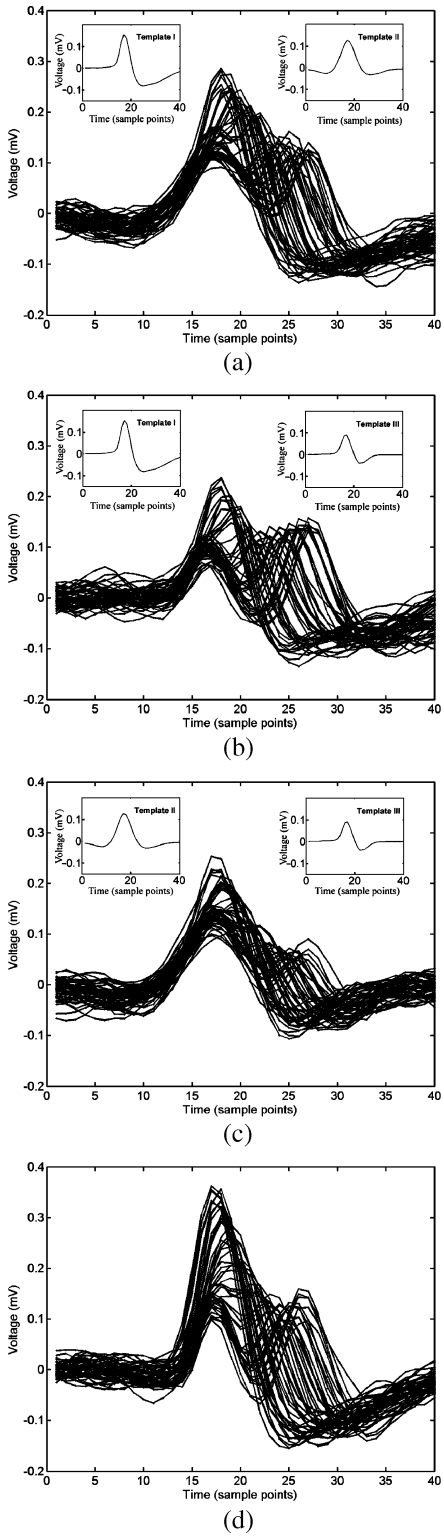

Fig. 1. Synthetic overlapping spikes ($\mathrm{SNR} = 2.5$). Each group contains fifty overlapped spikes. (a) Fifty overlapped spikes which are generated by superposing template I with delayed template II and background noise. (b) and (c) similar pictures for templates I/III and templates II/III, respectively. (d) Fifty overlapped spikes which are generated by superposing template I with delayed template II and III, and background noise.

estimated using those data that were in vicinities of the cluster centers being defined by spherical boundaries, so as to reduce the distortions that might be caused by the background noise. The results show that it

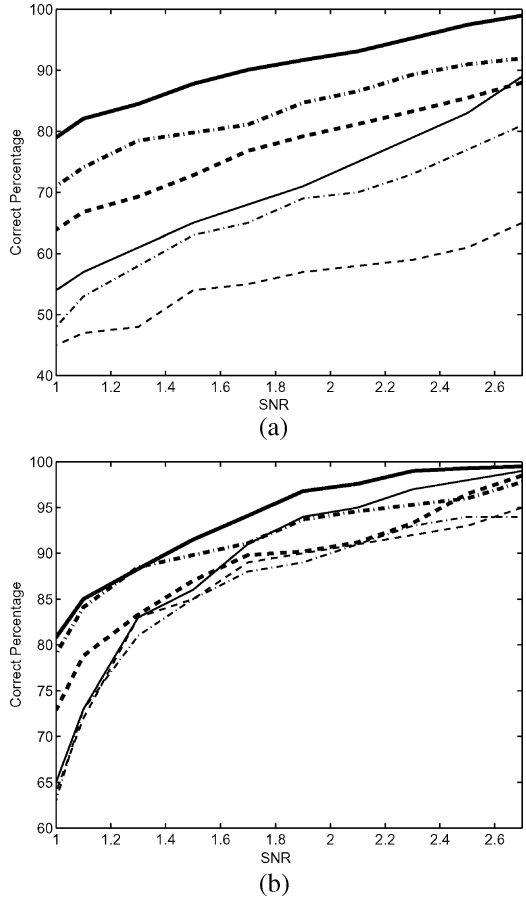

Fig. 2. The percentage of correct classification for single spikes (thick curves) and overlap (thin curves) decomposition (solid lines for our method, dashed lines for method [4] and dash-dotted lines for method [7]). (a) three-class case under various SNR levels. (b) two-class case under various SNR levels.

is feasible to use this proposed system, without any *a priori* knowledge about the background noise. Moreover, the proposed RELAX method achieved better performance than other methods [4], [7] in our application. However, there is still some limitation—the K-means algorithm is optimal classification method if the classes are normally distributed with spherical and equal covariance matrices, but it will cause suboptimal result if the noise deviates significantly from the above conditions.

ACKNOWLEDGMENT

The authors wish to thank Dr. R. Wu, Department of Electrical and Electronic Engineering at Imperial College London, and T. Li, Air China Technics for helpful discussions. They would also like to thank the reviewers of this manuscript for their helpful comments and suggestions.

REFERENCES

[1] E. N. Brown, R. E. Kass, and P. P. Mitra, "Multiple neural spike train data analysis: state-of-the- art and future challenges," *Nature Neurosci.*, vol. 7, pp. 456–461, 2004.

[2] M. S. Lewicki, "A review of methods for spike sorting: the detection and classification of neural action potential," *Netw.: Comput. Neural Syst.*, vol. 9, pp. R53–R78, 1998.

[3] M. S. Fee, P. P. Mitra, and D. Kleinfeld, "Variability of extracellular spike waveforms of cortical neurons," *J. Neurophysiol*, vol. 76, pp. 3823–3833, Dec. 1996.

[4] A. F. Atiya, "Recognition of multiunit neural signals," *IEEE Trans. Biomed. Eng.*, vol. 39, no. 7, pp. 723–729, Jul. 1992.

[5] P. M. Zhang, J. Y. Wu, Y. Zhou, P. J. Liang, and J. Q Yuan, "Spike sorting based on automatic template reconstruction with a partial solution to the overlapping problem," *J. Neurosci. Meth.*, vol. 135, pp. 55–65, 2004.

[6] M. S. Lewicki, "Bayesian modeling and classification of neural signals," *Neural Comp.*, vol. 6, pp. 1005–1030, 1994.

[7] I. N. Bankman, K. O. Johnson, and W. Schneider, "Optimal detection, classification, and superposition resolution in neural waveform recordings," *IEEE Trans. Biomed. Eng.*, vol. 40, no. 8, pp. 836–841, Aug. 1993.

[8] J. Li and P. Stoica, "Efficient mixed-spectrum estimation with applications to target feature extraction," *IEEE Trans. Signal Process.*, vol. 44, no. 2, pp. 281–295, Feb. 1996.

[9] P. Stoica and Y. Selen, " Cyclic minimizers, majorization techniques, and the expectation-maximization algorithm: a refresher," *IEEE Signal Process. Mag.*, vol. 21, no. 1, pp. 112–114, Jan. 2004.

[10] R. B. Wu and J. Li, "Time delay estimation with multiple looks in colored gaussian noise," *IEEE Trans. Aerosp. Electron. Syst.*, vol. 35, no. 4, pp. 1354–1361, Oct. 1999.

[11] K. H. Kim and S. J. Kim, "Neural spike sorting under nearly 0-dB signal-to-noise ratio using nonlinear energy operator and artificial neural-network classifier," *IEEE Trans. Biomed. Eng.*, vol. 47, no. 10, pp. 1406–1411, Oct. 2000.

[12] A. H. Chen, Y. Zhou, H. Q. Gong, and P. J. Liang, "Firing rates and dynamic correlated activities of ganglion cells both contribute to retinal information processing," *Brain Res.*, vol. 1017, pp. 13–20, 2004.

[13] R. J. Vogelstein, K. Murari, P. H. Thakur, C. Diehl, S. Chakrabartty, and G. Cauwenberghs, "Spike sorting with support vector machines," presented at the 26th Annu. Int. Conf. IEEE Engineering in Medicine and Biology Society, San Francisco, CA, Sep. 2004.

An Effective and Efficient Compression Algorithm for ECG Signals With Irregular Periods

Hsiao-Hsuan Chou*, Ying-Jui Chen, Yu-Chien Shiau, and Te-Son Kuo

***Abstract*—This paper presents an effective and efficient preprocessing algorithm for two-dimensional (2-D) electrocardiogram (ECG) compression to better compress irregular ECG signals by exploiting their inter- and intra-beat correlations. To better reveal the correlation structure, we first convert the ECG signal into a proper 2-D representation, or image. This involves a few steps including QRS detection and alignment, period sorting, and length equalization. The resulting 2-D ECG representation is then ready to be compressed by an appropriate image compression algorithm. We choose the state-of-the-art JPEG2000 for its high efficiency and flexibility. In this way, the proposed algorithm is shown to outperform some existing arts in the literature by simultaneously achieving high compression**

Manuscript received March 15, 2005; revised October 22, 2005. *Asterisk indicates corresponding author.*

*H.-H. Chou is with the Department of Electrical Engineering, National Taiwan University, Taipei 10617, Taiwan, R.O.C. (e-mail: hh.hhchou@gmail.com).

Y.-J. Chen is with the Department of Electrical Engineering, National Taiwan University, Taipei 10617, Taiwan, R.O.C. and also with the Intelligent Engineering Systems Laboratory, Massachusetts Institute of Technology, Cambridge, MA 02139 USA.

Y.-C. Shiau is with the Department of Nuclear Medicine, Far Eastern Memorial Hospital, Panchiao, Taipei 220, Taiwan, R.O.C.

T.-S. Kuo is with the Department of Electrical Engineering and the Institute of Biomedical Engineering, National Taiwan University, Taipei 10617, Taiwan, R.O.C. (e-mail: kuo@ntu.edu.tw).

Digital Object Identifier 10.1109/TBME.2005.863961